Hindawi Publishing Corporation
Advances in Materials Science and Engineering
Volume 2015, Article ID 376082, 6 pages
http://dx.doi.org/10.1155/2015/376082

Research Article

Radiolytic Synthesis of Colloidal Silver Nanoparticles for Antibacterial Wound Dressings

Pimpon Uttayarat, Jarurattana Eamsiri, Theeranan Tangthong, and Phiriyatorn Suwanmala

Thailand Institute of Nuclear Technology (Public Organization), 9/9 Moo 7, Tambon Saimoon, Ongkarak, Nakorn Nayok 26120, Thailand

Correspondence should be addressed to Pimpon Uttayarat; puttayar@alumni.upenn.edu

Received 4 July 2014; Accepted 27 August 2014

Academic Editor: Erwan Rauwel

Radiolytic synthesis provides a convenient and environmentally-friendly approach to prepare metallic nanoparticles in large scale with narrow size distribution. In this report, colloidal silver nanoparticles (AgNPs) were synthesized by gamma radiation using poly(vinyl alcohol) (PVA) or silk fibroin (SF) as stabilizers and were evaluated for their antibacterial properties. The conversion of metallic silver ions to silver atoms depended on irradiation dose and stabilizer concentration as determined by UV-Vis spectrophotometry and transmission electron microscopy. The uniformly dispersed AgNPs with diameter 32.3 ± 4.40 nm were evaluated as antiseptic agents in films composed of chitosan, SF, and PVA that were processed by irradiation-induced crosslinking. Using disc diffusion assay, the films containing 432 ppm AgNPs could effectively inhibit the growth of both *Staphylococcus aureus* and *Pseudomonas aeruginosa*. Therefore, we have demonstrated in our present study that gamma radiation technique can potentially be applied in the mass production of antibacterial wound dressings.

1. Introduction

Since ancient times, silver has been recognized for its medicinal use in wound treatment as well as its hygienic use in food and water preservation [1, 2]. During the past few decades, the antibacterial properties of silver become the center of research interest as several investigations have demonstrated the potent toxicity of silver against various Gram-positive and Gram-negative bacterial strains [1–7]. This allows silver to be used in a wide range of biomedical applications such as prevention of infection, wound healing, and anti-inflammation. A recent study also reported the ability of silver to synergistically enhance bactericidal activity of antibiotics against drug-resistant bacteria as well as biofilms in which the latter have become clinical challenges in treating chronic infections [2].

The advance in nanotechnology has driven the development of silver particles with nanometer size scale that yields many interesting properties that range from electronics to biomedical applications. The key synthesis aspects of silver nanoparticles (AgNPs) focus on the ability to control their size, shape, and dispersity [8]. Colloidal AgNPs can be prepared by the reduction of silver ion (Ag^+) precursor to their zero-valent (Ag^0) nuclei, which are stabilized by surfactants or polymers during the growth process to prevent agglomeration of large particles [3, 5, 8–10]. Various techniques have been reported in the synthesis of AgNPs including light-assisted reduction of Ag^+ by gamma radiation, UV radiation, laser ablation, and chemical reduction by reducing agents such as sodium borohydride, hydrazine, formaldehyde, ascorbic acid, and glucose [8–10]. Among these techniques, radiolytic synthesis by gamma radiation provides a major advantage for a large-scale production of monodisperse particles as it generates a uniform distribution of reducing agents in the entire solution during the irradiation process [9].

In the radiolytic synthesis of AgNPs, which was first developed by Henglein and Tausch-Treml [11], radiolysis of water generates active species such as hydrated electrons and hydroxyl radicals [9–12]:

$$H_2O \xrightarrow{\gamma\text{-ray}} e^-_{aq}, H^\bullet, OH^\bullet, H_2, H_3O^+, \ldots \quad (1)$$

$$Ag^+ + e^-_{aq} \longrightarrow Ag^0. \quad (2)$$

Hydrated electrons directly reduce Ag^+ precursor to Ag^0 nuclei, which progressively coalesce into clusters. To prevent hydroxyl radicals from oxidizing nascent Ag^0 clusters, scavengers such as alcohols are usually added prior to the irradiation process [9, 10] to react with the hydroxyl radicals. This results in the formation of hydroxyalkyl radicals which in turn react with other molecules in solution to produce new radicals for the reduction of Ag^+ to Ag^0 [9].

To ensure the dispersion of AgNPs in aqueous solution, polymers containing functional groups such as $–NH_2$, –COOH, and –OH are added as stabilizers during the irradiation process [5, 12]. Due to their high affinity for silver, these polymers anchor on the surface of AgNPs, providing electrostatic repulsion and steric hindrance [12] that prevent rapid agglomeration of small clusters into large particles. Previous studies have reported the use of both natural and synthetic polymers such as chitosan, gelatin, carboxymethyl cellulose, poly(vinyl alcohol) (PVA), and polyvinylpyrrolidone (PVP) as stabilizers [3, 5, 10]. The resulting AgNPs are shown to be monodisperse with size that ranged from a few to tens of nanometers [3, 5, 10, 12, 13].

In biomedical application, wound dressings possessing hydrogel and antimicrobial properties are desirable as coverage over wounds to absorb exudates and prevent bacterial infection, thus promoting the regeneration of skin tissue and wound healing [7, 14]. Naturally derived polymers such as silk fibroin (SF) from cocoons of silkworms and chitosan (CS) from chitin of crustaceans have recently attracted considerable attention as a choice of materials for the fabrication of wound dressings due to their biocompatibility, water absorption, and excellent mechanical properties [15–17]. In this report, colloidal AgNPs were prepared by radiolytic synthesis and evaluated as an antiseptic agent when incorporated into dressing films. In the irradiation-induced reduction process, we tested SF protein as stabilizer in comparison to PVA. The morphology and dispersion of nanoparticles were shown to depend on irradiation dose and stabilizer concentration. Disc diffusion assay showed that SF-CS-PVA films embedded with AgNPs could effectively inhibit bacterial growth.

2. Materials and Method

2.1. Radiolytic Synthesis of Colloidal AgNPs. Silver nitrate ($AgNO_3$, Merck, Germany) was used as the starting source of silver for the radiolytic-induced reduction of Ag^+ to Ag^0. Commercial PVA (M_w 72.000, Merck, Germany) and SF protein (molecular weight ~ 20–238 kDa) extracted from cocoons of silkworm *Bombyx mori* using the previously described method [7] were used as stabilizers. Reversed osmosis water was used to prepare solutions in all experiments. Solutions containing 40 mM $AgNO_3$ were prepared in 0.5, 1, and 2% (w/v) PVA (M_w 72.000, Merck, Germany) with 0.8 M ethanol or in 0.5, 1, 2, and 5% (w/v) SF. After deaeration by bubbling with nitrogen gas, the solutions were irradiated by gamma rays from a Co-60 source (gammacell 220) at doses 0, 20, 40, and 60 kGy and a dose rate of 4.98 kGy/h.

2.2. Characterization of Colloidal AgNPs. The formation, morphology, and dispersion of colloidal AgNPs were determined to obtain the optimal dose and stabilizer concentration for the irradiation process. UV-Vis spectrophotometry was used to determine the presence of AgNPs which showed a characteristic absorption peak of Ag^0 distinctive from the starting Ag^+. After the irradiation process, solutions containing colloidal AgNPs at all treatments were diluted by water to 0.16 mM calculated per the starting $AgNO_3$ solution and the UV-Vis spectra were recorded by a spectrophotometer (Evolution 300, Thermo Scientific). The morphology and dispersion of AgNPs were examined by transmission electron microscopy (TEM, Hitachi HT7700). The diameters of AgNPs were measured from ~50 particles for treatments that yielded the uniform dispersion of particles and were represented as mean ± standard deviation.

2.3. Preparation of SF-CS-PVA Wound Dressing Films. A 2% (w/v) CS solution was first prepared in 1% (v/v) acetic acid and the pH was adjusted to 6.5. Subsequently, 2% (w/v) SF powder was added to the CS solution and stirred overnight at RT until completely dissolved. The mixed SF-CS solution was concentrated into a paste-like form by rotor evaporation before a 15% (w/v) PVA solution was added into the paste to obtain the final concentration of 20, 33, 50, and 67% (w/w). After being thoroughly mixed by stirring, the paste was cast into 5 cm × 7 cm × 0.1 cm Teflon molds and rendered crosslinked by exposure to gamma rays from a Co-60 source (Gems Irradiation Center, Thailand Institute of Nuclear Technology (Public Organization)) for a total dose of 80 kGy at a dose rate of 9.52 kGy/h. For the evaluation of antibacterial properties, AgNPs at varied concentrations were added to the selected paste formulation prior to gamma irradiation.

2.4. Characterization of SF-CS-PVA Films. Using universal testing machine (Cometech, B2-type), the mechanical properties including elastic modulus, stress at break, and strain at break of SF-CS-PVA films were determined. Samples were cut into 1 cm × 4 cm strips and mounted on 50 N load cell that moved at a speed of 50 mm/min. Data were collected as load and displacement from 3–5 samples per PVA concentration. The elastic modulus was calculated from stress-strain curves.

In addition to the mechanical properties, the ability of films to absorb water was determined by the degree of swelling. Samples were incubated in 1X phosphate buffer saline (1X PBS) containing calcium and phosphate ions at 37°C for 72 h, blotted with kimwipes paper and weighed. The degree of swelling was calculated according to the following formula [18]:

$$\text{Degree of swelling}\,(\%) = \frac{W_s - W_d}{W_d} \times 100, \tag{3}$$

where W_s is the weight of film in its swollen state and W_d is the film's dry weight. Films with optimal SF-CS-PVA formulation were chosen as the wound dressing model for the evaluation of antibacterial properties.

2.5. Evaluation of Antibacterial Properties. The ability of colloidal AgNPs to serve as antiseptic agent was evaluated by disc diffusion assay at varied AgNPs concentrations from 0 to 2.160 ppm. To confirm the presence of AgNPs,

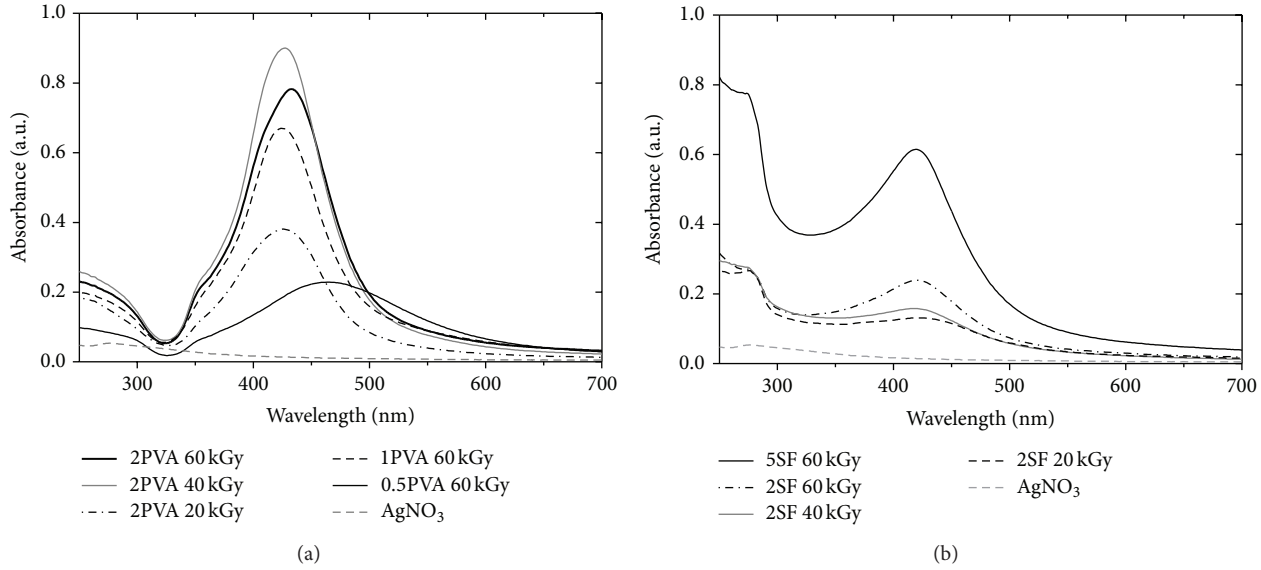

Figure 1: UV-Vis spectra of colloidal AgNPs synthesized by gamma radiolysis with (a) PVA or (b) SF as stabilizers at different irradiation doses and stabilizer concentrations.

AgNP-embeded films were inspected by scanning electron microscopy (SEM, JOEL JSM 6380 LV) and the presence of Ag was analyzed by energy dispersive X-ray spectrometer (EDS). Films were cut into circular discs 8 mm in diameter, placed on Mueller-Hinton agar plates that were preinoculated with 10^6 colony forming unit (CFU)/mL of either *S. aureus* or *P. aeruginosa* and incubated at 37°C for 18 h. The clear zones surrounding the discs, which indicated inhibition of bacterial growth, were recorded at the termination of incubation period and the inhibition ratios were calculated as the average diameters of zones of inhibition divided by the disc diameters. Data were represented as mean ± standard deviation from 8 replicates.

3. Results and Discussion

3.1. Effect of Irradiation Dose on the Formation of Colloidal AgNPs. After exposure to gamma irradiation, the formation of colloidal AgNPs in solutions could be observed by changes in color of the starting $AgNO_3$ from clear to reddish brown for AgNPs stabilized by PVA and dark brown for AgNPs stabilized by SF. For well dispersed AgNPs with size of a few nanometers, the optical property determined by UV absorption exhibits an intense peak characteristic to Ag^0 at wavelengths 380–440 nm as reported in previous studies [5, 8, 10–12]. Here we first tested the effect of irradiation dose on the formation of colloidal AgNPs.

At the highest PVA concentration (2PVA, Figure 1), the presence of AgNPs was indicated by UV-Vis spectra which showed the maximum absorption wavelength (λ_{max}) at 425–432 nm. As an internal control, the absorption band was absent in the spectra of $AgNO_3$. The highest absorbance intensity was obtained at irradiation dose of 40 kGy with a slight shift towards shorter wavelength. For colloidal AgNPs capped with SF (Figure 1(b)), λ_{max} at 420 nm was distinct when the irradiation dose was raised to 60 kGy, whereas it almost diminished at lower doses. Table 1 summarizes UV absorption data of AgNPs at all irradiation doses and stabilizer concentrations tested in this present study.

Table 1: Effect of irradiation dose and stabilizer concentration on the UV absorption of colloidal AgNPs.

Stabilizer (% w/v)	Dose (kGy)	λ_{max} (nm)	Absorbance (a.u.)
0.5PVA	20	447	0.177
0.5PVA	40	432	0.316
0.5PVA	60	463	0.229
1PVA	20	424	0.307
1PVA	40	419	0.451
1PVA	60	421	0.57
2PVA	20	425	0.381
2PVA	40	427	0.901
2PVA	60	432	0.783
2SF	20	415	0.131
2SF	40	414	0.158
2SF	60	419	0.239
5SF	20	421	0.206
5SF	40	419	0.4
5SF	60	419	0.615

Note: UV-Vis spectra could not be observed for AgNPs prepared in SF solutions at concentrations below 1% (w/v).

The morphology of AgNPs was further examined by TEM. For AgNPs capped with 2% (w/v) PVA, large aggregates surrounded by small particles (diameter ~ 28 nm) formed at irradiation dose of 20 kGy, whereas a uniform dispersion of individual, small particles with diameters 32.3 ± 4.40 and 41.1 ± 4.00 nm was obtained at doses 40 and 60 kGy, respectively. The slight increase in particle size at higher irradiation dose may be due to degradation of PVA, which could be less effective in preventing the growth of particles.

Table 2: The mechanical properties and degree of swelling of SF-CS-PVA films at varied PVA concentration. Data are represented as mean ± standard deviation.

% PVA (w/w)	Stress at break (kPa)	Strain at break (%)	Elastic modulus (kPa)	Degree of swelling (%)
20	109.6 ± 40.3	18.0 ± 3.4	1111.6 ± 415.9	134.15 ± 2.72
33	313.8 ± 35.0	27.8 ± 2.4	1960.5 ± 160.2	131.37 ± 1.98
50	346.2 ± 39.9	36.8 ± 4.6	2567.3 ± 288.8	148.80 ± 3.11
67	374.1 ± 28.82	68.9 ± 4.3	2242.7 ± 493.5	166.27 ± 2.33

This observation is similar to the previous report of chitosan-capped AgNPs prepared at high irradiation dose [10]. For AgNPs capped with SF, large aggregates as well as small particles were observed at the irradiation dose of 60 kGy. Interestingly, these small particles (diameter ~ 40 nm, Figure 2(d)) remained connected and were not fully dispersed. This can be attributed to the less hydrated nature of SF protein compared to PVA that makes it less effective in shielding individual particles apart from each other. Based on these data, the extent of irradiation dose in our experimental conditions plays a major role in the formation of small Ag^0 particles.

3.2. Effect of Stabilizer Concentration on the Formation of Colloidal AgNPs. Agglomeration of Ag^0 into large particles can be prevented by stabilizers that envelop over the particle surface. In this report, PVA and SF at varied concentrations were tested to optimize the morphology and dispersion of AgNPs. At the same irradiation dose of 60 kGy, the UV-Vis spectra showed narrower absorption bands with shifts towards shorter wavelength and higher peak intensity as the PVA concentrations increased from 0.5 to 2% (w/v) (Figure 1(a)). These changes may correspond to the formation of smaller particles with narrow distribution in particle size [10] as the red shifts and broadening of the band are due to agglomeration of Ag^0 into large clusters [5]. Similarly for AgNPs capped with SF, the absorption band with strongest peak intensity corresponded to AgNPs prepared in 5% (w/v) SF solution (Figure 1(b)), whereas AgNPs prepared with lower SF concentrations contributed to absorption bands with lower intensities.

In line with UV-Vis spectra, the majority of particles were in large aggregates (Figure 2(e)) at the lowest PVA concentration, whereas a mix of large aggregates and small particles was observed at 1.0% (w/v) PVA (Figure 2(f)) and the uniform dispersion of AgNPs was obtained at 2% (w/v) PVA (Figures 2(b) and 2(c)). Thus, a sufficient concentration of PVA was required to prevent particle agglomeration. Taken all together, both the irradiation dose and PVA concentration affect the formation and dispersion of Ag^0 into small, individual particles in our study. Based on the morphology and uniform dispersion of colloidal AgNPs, we selected AgNPs prepared with 2% (w/v) PVA at irradiation dose of 40 kGy to be incorporated into dressing films for the evaluation of antibacterial properties.

3.3. Characterization of SF-CS-PVA Films. Using radiation processing technique, polymeric films can be crosslinked and simultaneously sterilized in a single step [19], which is advantageous for the fabrication of biomedical products. In this report, we also utilized gamma radiation to process wound dressing films composed of SF, CS, and PVA. The optimal formulation of SF-CS-PVA films was chosen based on the films' mechanical and swelling properties as summarized in Table 2. In terms of the mechanical properties, the stress at break, strain at break and elastic modulus were shown to increase with the PVA concentration. As the proportion of PVA was raised to more than 50% (w/w), the elastic modulus and stress at break did not change significantly although the strain at break continued to increase with PVA concentration.

The ability to absorb fluid is one of the key aspects of wound dressing, which can be characterized by the degree of swelling. Our data showed that the degrees of swelling of SF-CS-PVA films at all PVA concentrations were more than 100% with a slight increase with PVA concentration. These values were in agreement with other PVA-based hydrogels in previous report [20]. Based on these data, the formulation of the film was selected to comprise 50% PVA (w/w), which possessed the highest content of natural polymer components while still maintaining the optimal mechanical and swelling properties.

3.4. Inhibition of Bacterial Growth. The SF-CS-PVA films incorporated with AgNPs at concentrations 0–2.160 ppm were evaluated for antibacterial properties against *S. aureus* and *P. aeruginosa* by disc diffusion assay. The distribution of AgNPs throughout the film was confirmed by EDS signals taken over the cross-sectional area of the film (Figure 3). Prominent clear areas (Figure 4), indicating the zones of growth inhibition, around the films on plates inoculated with either bacterial strain were observed when AgNP concentration was raised ≥432 ppm and increased with the amount of AgNPs in the films. As an internal control, no clear zone was observed around films without AgNPs.

For *S. aureus*, the inhibition ratios, calculated as the average diameters of zones of inhibition divided by the disc diameters, increased from 1.46 ± 0.14 at 432 ppm AgNPs to 1.67 ± 0.18 at 2160 ppm AgNPs. Similarly, the inhibition ratios for *P. aeruginosa* were 1.44 ± 0.16 and 1.59 ± 0.19 at 432 ppm and 2160 ppm AgNPs, respectively. In our study, the minimum concentration of AgNPs in the films that exhibited antibacterial properties against both strains of bacteria was less than the amount of Ag compounds used in some commercial wound dressings [7]. Therefore, we have demonstrated that colloidal AgNPs can serve as an effective

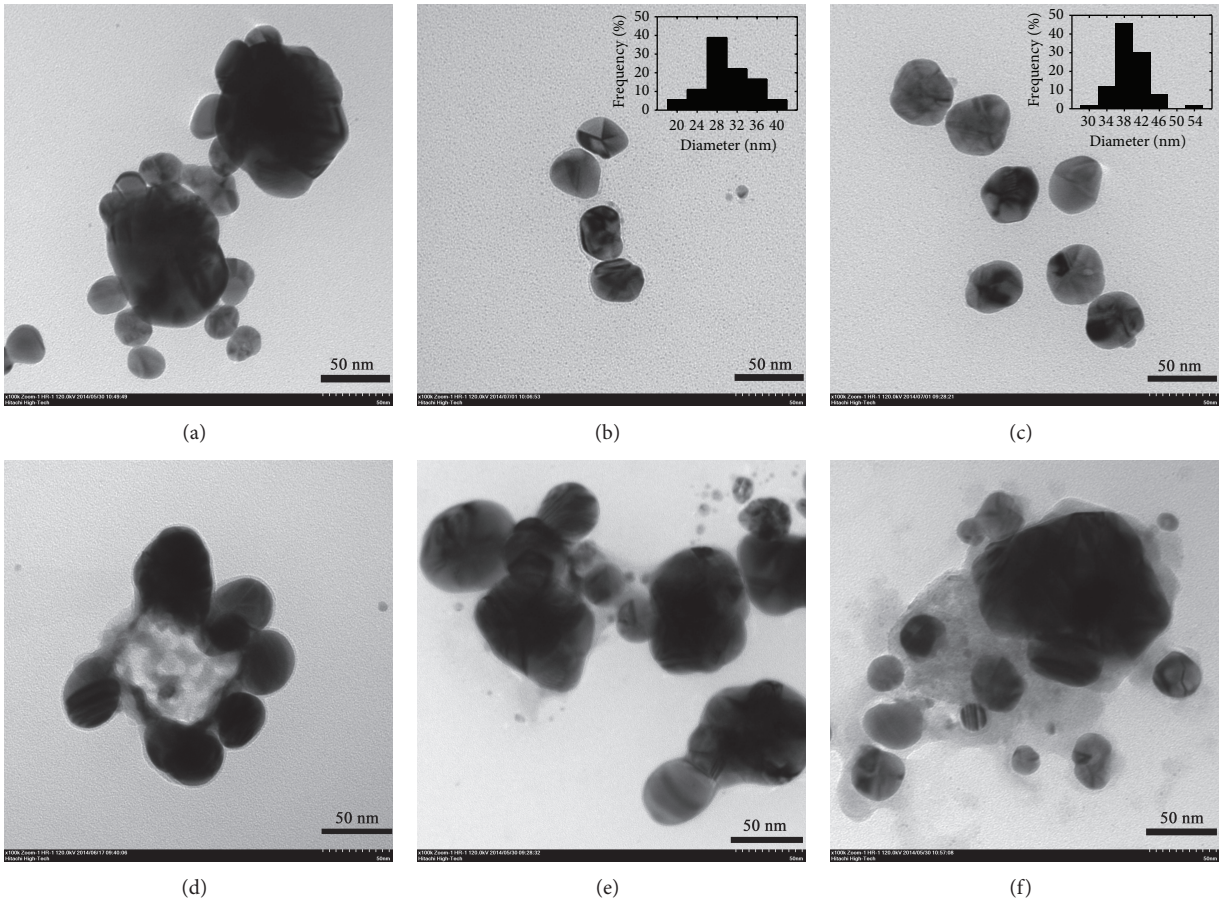

Figure 2: TEM images representing the morphology and dispersion of colloidal AgNPs. Top panel are images of AgNPs prepared in 2% (w/v) PVA solutions at irradiation doses of (a) 20, (b) 40, and (c) 60 kGy. Insets show histograms of size distribution. In lower panels, AgNPs were formed at the irradiation dose of 60 kGy in (d) 5% (w/v) SF, (e) 0.5% (w/v) PVA, and (f) 1.0% (w/v) PVA solutions.

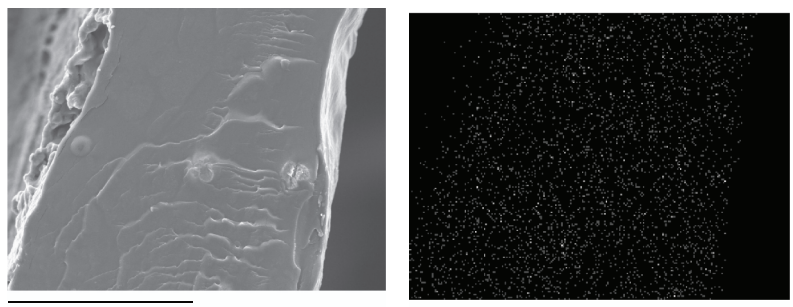

Figure 3: Representative SEM images show (a) the cross-section of SF-CS-PVA film incorporated with AgNPs at a concentration of 2,160 ppm and (b) collected EDS signal of silver over the cross-sectional area.

antiseptic agent when incorporated into films, which can potentially be used in wound healing application.

4. Conclusion

Gamma radiation was applied in the radiolytic synthesis of colloidal AgNPs and processing of films for wound dressing application. The size and dispersion of particles were shown to depend on the irradiation dose and concentration of stabilizer in which the uniform dispersion of AgNPs with size in the range of 30–40 nm was achieved at doses ≥40 kGy and 2% (w/v) PVA. When incorporated into SF-CS-PVA films, the concentration of AgNPs at 432 ppm was found to be effective in inhibiting the growth of bacteria.

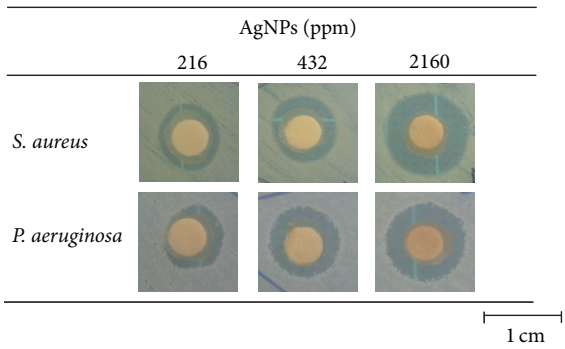

Figure 4: Disc diffusion assay shows the antibacterial properties of SF-CS-PVA films embedded with AgNPs. The inhibition of bacterial growth appears as clear zones surrounding the films.

Conflict of Interests

The authors declare that there is no conflict of interests regarding the publication of this paper.

Acknowledgments

This project was sponsored by the Thailand Institute of Nuclear Technology (Public Organization) (TINT) and the Thai National Research Center. The authors thanked the staff members at the Gems Irradiation Center, TINT for their help on experiments involving the use of gamma radiation facility. The authors also thank Ms. Patcharee Saechua and Ms. Pantip Boonlue for their help in the extraction of silk and other technical works in the laboratory.

References

[1] S. Silver, L. T. Phung, and G. Silver, "Silver as biocides in burn and wound dressings and bacterial resistance to silver compounds," *Journal of Industrial Microbiology and Biotechnology*, vol. 33, no. 7, pp. 627–634, 2006.

[2] J. R. Morones-Ramirez, J. A. Winkler, C. S. Spina, and J. J. Collins, "Silver enhances antibiotic activity against gram-negative bacteria," *Science Translational Medicine*, vol. 5, no. 190, Article ID 190ra81, 2013.

[3] A. G. Hassabo, A. A. Nada, H. M. Ibrahim, and N. Y. Abou-Zeid, "Impregnation of silver nanoparticles into polysaccharide substrates and their properties," *Carbohydrate Polymers*, 2014.

[4] I. Sondi and B. Salopek-Sondi, "Silver nanoparticles as antimicrobial agent: a case study on *E. coli* as a model for Gram-negative bacteria," *Journal of Colloid and Interface Science*, vol. 275, no. 1, pp. 177–182, 2004.

[5] D. van Phu, V. T. K. Lang, N. T. K. Lan et al., "Synthesis and antimicrobial effects of colloidal silver nanoparticles in chitosan by γ-irradiation," *Journal of Experimental Nanoscience*, vol. 5, no. 2, pp. 169–179, 2010.

[6] Q. L. Feng, J. Wu, G. Q. Chen, F. Z. Cui, T. N. Kim, and J. O. Kim, "A mechanistic study of the antibacterial effect of silver ions on *Escherichia coli* and *Staphylococcus aureus*," *Journal of Biomedical Materials Research*, vol. 52, pp. 662–668, 2000.

[7] P. Uttayarat, S. Jetawattana, P. Suwanmala, J. Eamsiri, T. Tangthong, and S. Pongpat, "Antimicrobial electrospun silk fibroin mats with silver nanoparticles for wound dressing application," *Fibers and Polymers*, vol. 13, no. 8, pp. 999–1006, 2012.

[8] K.-M. Cheng, Y.-W. Hung, C.-C. Chen, C.-C. Liu, and J.-J. Young, "Green synthesis of chondroitin sulfate-capped silver nanoparticles: characterization and surface modification," *Carbohydrate Polymers*, vol. 110, pp. 195–202, 2014.

[9] M. Grzelczak and L. M. Liz-Marzán, "The relevance of light in the formation of colloidal metal nanoparticles," *Chemical Society Reviews*, vol. 43, no. 7, pp. 2089–2097, 2014.

[10] P. Chen, L. Song, Y. Liu, and Y. E. Fang, "Synthesis of silver nanoparticles by γ-ray irradiation in acetic water solution containing chitosan," *Radiation Physics and Chemistry*, vol. 76, no. 7, pp. 1165–1168, 2007.

[11] A. Henglein and R. Tausch-Treml, "Optical absorption and catalytic activity of subcolloidal and colloidal silver in aqueous solution: a pulse radiolysis study," *Journal of Colloid And Interface Science*, vol. 80, no. 1, pp. 84–93, 1981.

[12] M. K. Temgire and S. S. Joshi, "Optical and structural studies of silver nanoparticles," *Radiation Physics and Chemistry*, vol. 71, no. 5, pp. 1039–1044, 2004.

[13] B.-S. Liu and T.-B. Huang, "Nanocomposites of genipin-crosslinked chitosan/silver nanoparticles—structural reinforcement and antimicrobial properties," *Macromolecular Bioscience*, vol. 8, no. 10, pp. 932–941, 2008.

[14] A. Sugihara, K. Sugiura, H. Morita et al., "Promotive effects of a silk film on epidermal recovery from full-thickness skin wounds," *Proceedings of the Society for Experimental Biology and Medicine*, vol. 225, no. 1, pp. 58–64, 2000.

[15] R. A. A. Muzzarelli, "Genipin-crosslinked chitosan hydrogels as biomedical and pharmaceutical aids," *Carbohydrate Polymers*, vol. 77, no. 1, pp. 1–9, 2009.

[16] G. H. Altman, F. Diaz, C. Jakuba et al., "Silk-based biomaterials," *Biomaterials*, vol. 24, no. 3, pp. 401–416, 2003.

[17] L. Zhao and H. Mitomo, "Hydrogels of dihydroxypropyl chitosan crosslinked with irradiation at paste-like condition," *Carbohydrate Polymers*, vol. 76, no. 2, pp. 314–319, 2009.

[18] Y. C. Nho and K. R. Park, "Preparation and properties of PVA/PVP hydrogels containing chitosan by radiation," *Journal of Applied Polymer Science*, vol. 85, no. 8, pp. 1787–1794, 2002.

[19] M. Haji-Saeid, A. Safrany, M. H. D. O. Sampa, and N. Ramamoorthy, "Radiation processing of natural polymers: the IAEA contribution," *Radiation Physics and Chemistry*, vol. 79, no. 3, pp. 255–260, 2010.

[20] B. B. Mandal, A. S. Priya, and S. C. Kundu, "Novel silk sericin/gelatin 3-D scaffolds and 2-D films: fabrication and characterization for potential tissue engineering applications," *Acta Biomaterialia*, vol. 5, no. 8, pp. 3007–3020, 2009.